Journal of Theoretical Biology 307 (2012) 29–36

Contents lists available at SciVerse ScienceDirect

Journal of Theoretical Biology

journal homepage: www.elsevier.com/locate/yjtbi

Predation on infected host promotes evolutionary branching of virulence and pathogens' biodiversity

Andrew Morozov [a,*], Alex Best [b,c]

[a] Department of Mathematics, University of Leicester, LE1 7RH, UK
[b] School of Mathematics and Statistics, University of Sheffield, Sheffield, S3 7RH, UK
[c] Biosciences, College of Life and Environmental Sciences, University of Exeter Cornwall Campus, Penryn TR10 9EZ, UK

HIGHLIGHTS

- We investigate the role of predators in biodiversity of the pathogens of prey.
- The study is based on principles of adaptive dynamics and evolutionary game theory.
- Predation on infected host can result in evolutionary branching of pathogens.
- Predator-mediated dimorphism occurs within large ranges of life-history traits.

ARTICLE INFO

Article history:
Received 12 November 2011
Received in revised form
5 March 2012
Accepted 17 April 2012
Available online 9 May 2012

Keywords:
Evolutionary branching
Virulence evolution
Ecoepidemiology
Polymorphism

ABSTRACT

Traditionally, theoretical works on the evolution of virulence of wildlife infections have focused on interactions between just the host and its parasite. In a large number of study cases, however, infected host individuals also incur severe mortality due to predation of higher trophic levels. Such mortality should be virulence-dependent since the population size of predators is determined by the available amount prey they consume, which, in turn, is a function of pathogen virulence. The potential role of trophic pressure by predators in the evolution of virulence of their prey remains largely unaddressed in the literature. Here we investigate the possible role of predators in promoting biodiversity and disruptive evolution (evolutionary branching) of pathogen strains infecting the prey that those predators consume. Our theoretical study is based on principles of adaptive dynamics and evolutionary game theory. With the help of a fairly simple model we demonstrate that predation on infected prey can result in evolutionary branching of pathogen virulence, which would be impossible in the same system without predators. We show that predator-mediated evolutionary branching can occur within a large range of species life-history traits and for various types of transmission–virulence trade-off relation. We argue that predation can play an important role in explaining the existing polymorphism and biodiversity of pathogen strains in wildlife.

1. Introduction

The evolution of parasite virulence in natural populations has long been the focus of both theoretical and experimental studies (Anderson and May, 1982; Bremermann and Pickering, 1983; Taylor et al., 1998; Day and Proulx, 2004; Duffy and Sivars-Becker, 2007; Friman et al., 2009). Most of this previous work has been limited to examining only the interactions between the host and its parasite. In wildlife, however, species will often simultaneously be under pressure from both pathogens and predators. Furthermore, since diseased prey may be easier to catch than healthy individuals, in many cases predators will mostly consume infected prey (Friend, 2002; Packer et al., 2003; Johnson et al., 2006; Duffy and Sivars-Becke, 2007). Thus, infected host individuals may incur severe mortality costs via both predation and disease virulence. Given that these combined pressures are likely to affect the selection pressure on the parasite, it is important to understand the impact of predation on the resulting outcome of virulence evolution and its epidemiological consequences.

It is well understood in the theoretical literature that the level of background (non-disease induced) mortality plays an important role in the evolution of virulence (Anderson and May, 1982; Elbert and Weisser, 1997; Dieckmann, 2002; Pugliese, 2002). Clearly, in natural communities a significant proportion of such background mortality is likely to be caused by predation. Furthermore, this predation-caused mortality cannot be assumed to be

* Corresponding author. Tel.: +44 7 495 124 5983.
E-mail address: morozov_andrew@yahoo.com (A. Morozov).

0022-5193/$ - see front matter © 2012 Elsevier Ltd. All rights reserved.
http://dx.doi.org/10.1016/j.jtbi.2012.04.023

constant, since the population size of predator(s) is determined by the abundance of prey in the system, which, in turn, depends on the pathogen virulence. As a result, the predation-caused mortality becomes a function of pathogen virulence. There are therefore likely to be complicated inter-dependenices between parasitism and predation, the consequences of which may only be fully understood through the analysis of theoretical models.

The effect of predation on virulence evolution is almost entirely unaddressed in the theoretical literature. In two exceptions, Choo et al. (2003) and Morozov and Adamson (2011) have shown based on adaptive dynamics framework that adding predators into host–pathogen systems can both increase and decrease the evolutionarily stable level of virulence, and also that the presence of a predator can result in evolutionary suicide in the parasite. In this paper, we address another important issue by considering the potential role of trophic pressure in the emergence and coexistence of multiple viral strains in wild systems. Recent theory has found a variety of mechanisms that allow for evolutionary branching in the parasite, resulting in a polymorphism of strains with different levels of virulence. Possible mechanisms are non-linear mortality of infected hosts (Pugliese, 2002; Svennungsen and Kisdi, 2009, Best et al., 2009), specialist parasitism amongst multiple types of hosts (Regoes et al., 2000; Gudelj et al., 2004; Best et al., 2010) and superinfection (Adler and Mosquera, 2002; Boldin and Diekmann, 2008). In all of these cases, the potential for branching has been found to depend critically on the shape of the trade-off between transmission and virulence. It is therefore important that we understand the effect of this trade-off on the possible evolutionary outcomes predicted by models (de Mazancourt and Dieckmann, 2004; Rueffler, 2004; Bowers et al., 2005).

In this study, we consider a classical susceptible–infected (SI) host–parasite model with the addition of a generalist predator consuming infected hosts. We assume that the probability that predator catches prey individuals infected with more virulent parasites is higher compared to individuals infected by strains with lower virulence; this signifies a higher attack rate on prey infected with more virulent parasites (Choo et al., 2003). We are mainly interested in the possibility of evolutionary branching of virulence in this system. We show that the addition of the selective predator allows for evolutionary branching in parasite virulence. Interestingly, in the absence of predation (SI system), evolutionary branching does not occur, thus the branching becomes predation-mediated. We show that this polymorphism can occur for a large range of model parameters characterizing species life-history traits. We analyze the potential influence of the environment on the possibility of evolutionary branching by varying the carrying capacity and the prey birth rate thus simulating eutrophic and oligotrophic environments. Our main conclusion is that predation on infected hosts in natural populations should play a role in diversification of pathogen strains.

2. The model

We consider an SI model combined with a Rosenzweig–MacArthur predator–prey model. The system's dynamics are given by the following differential equations:

$$S' = r\left(1-\frac{S+I}{K}\right)S-\lambda SI, \tag{1}$$

$$I' = (\lambda S-D_0-D-mP)I, \tag{2}$$

$$P' = (kmI-\delta)P, \tag{3}$$

where the state variables describe densities of healthy (S) and infected (I) subpopulations of the prey and P is the density of predator. We assume that the predator (P) only consumes infected prey individuals, which is a rather typical scenario observed both in field and laboratory observations (Kabata, 1985; Holmes and Zohar, 1990; Hudson et al., 1992, 1998; Friend, 2002; Johnson et al., 2006; Duffy and Sivars-Becke, 2007). The parameters K (the carrying capacity) and r (the intrinsic *per capita* birth rate) characterize the growth rate of the prey population in the absence of predation. For the sake of simplicity, we assume that there is no saturation in predation (Holling type I functional response), the parameter m being the attack rate. The parameters k and δ are, respectively, the trophic efficiency coefficient and the natural mortality of the predator. The predator-independent part of the mortality of infected prey is the sum of the background mortality, D_0, and the disease-induced mortality D, which we shall henceforth refer to as the virulence of the disease. We describe transmission of the disease via the mass action term λSI, where the coefficient λ is called the transmission coefficient.

The dynamics of model (1)–(3) on a population (non-evolutionary) time scale, where all life traits of species are constant, is rather simple. In the case where the interior coexistence equilibrium exists (with all species densities being positive) it is always globally stable (see Appendix A for details). Thus, on a short time scale, all species densities will be close to their equilibrium values, which in turn depend on the current value of virulence D.

We consider that the model parameters m and λ are functions of the virulence D, i.e. $m=m(D)$ and $\lambda=\lambda(D)$. The assumption that the transmission rate and the virulence are related via a trade-off function has both theoretical and experimental background (see Alizon et al. (2009) for a review) and is frequently used in evolutionary models. The broad assumption is that increased within-host growth by the parasite aids transmission but also causes increased damage to the host. The assumption that the attack rate on the infected prey can be a function of the disease virulence is equivalent to the suggestion that a more severe disease strain would make the infected individual more vulnerable to predation than a more benign strain (Choo et al., 2003).

The choice of the particular trade-off relation is of crucial importance. Indeed, it was shown in a number of publications that the evolutionary outcome may strongly depend on the choice of the shape of the trade-off function (de Mazancourt and Dieckmann, 2004; Hoyle et al., 2008; Svennungsen and Kisdi, 2009). On the other hand, it is rather hard to reveal the real trade-off relation between the virulence based on experiments/observations (Alizon et al., 2009). To overcome this difficulty, at least partially, we implement here a geometrical approach to show which conditions (in terms of local derivatives of the trade-off functions $m(D)$ and $\lambda(D)$) are necessary to have evolutionary branching in the system, namely trade-off and invasion plots (TIPs). The theoretical basis for this approach is given in Bowers et al. (2005) and is partially explained in the next section. Implementation of a geometrical approach will allow us to extend our analysis to a family of trade-off functions and to not restrict ourselves to a particular mathematical expression (e.g., the hyperbolic trade-off function commonly used in the literature). Here we only require a few constrains for $m(D)$ and $\lambda(D)$ regarding local properties of those functions. In particular, for $\lambda(D)$ and $m(D)$ we require that those functions should be positive functions increasing with D (i.e. prey infected by a more virulent strain can be caught more easily).

Investigation of the evolutionary outcomes is done based on the theoretical methods of adaptive dynamics and game theory (Metz et al., 1992; Geritz et al., 1998; Dieckmann, 2002). In particular, we compute the invasion fitness of a rare mutant,

defined as its growth rate when rare, with slightly different virulence which is introduced into the system with population densities being at equilibrium; a successful invasion would correspond to a positive fitness of the invader. On an evolutionary time scale the disease strain will evolve in the direction of the local selection gradient until it reaches an evolutionary singularity, where the selection gradient vanishes. The further behavior will depend on the stability conditions of the given singular point. Note that the existence and stability of evolutionary singularities ('stopping points') depends on the shape of the trade-off function (Geritz et al., 1998). Here we will be focusing on finding evolutionary branching points of the system. These are convergence stable (locally attracting) but evolutionarily unstable (local fitness minima) singular points. As such selection will drive the population towards this point, but once there will undergo disruptive selection and branch into two coexisting strains.

3. Evolutionary behavior of the model

In this section we investigate the evolutionary behavior of the system at its singularity, where the selection gradient vanishes. We implement a TIP (trade-off and invasion plot) technique which provides a geometric interpretation of adaptive dynamics theory (Bowers et al., 2005; Hoyle et al., 2008). TIPs allow us to explore how the evolutionary behavior at a chosen singular point is dependent on the choice of trade-off between transmission and virulence. By implementing this technique, we therefore state that the given parameters (λ, D) already correspond to an evolutionarily singular strategy, where the invasion fitness of any mutant is zero (zero selection gradient). We are interested in revealing the shape of trade-off functions passing through this point which would guarantee branching behavior. The given singularity can be an evolutionary attractor where the virulence evolves to this point and remains there (the local invasion fitness has its maximum). Another situation is where the virulence will eventually evolve away from this point (evolutionary repeller). Finally, we can have the situation where the virulence evolves to the singularity having a minimal fitness. In this case, the evolutionary singular point is a *branching point* resulting in the establishment of two independent strains with further divergence in the evolutionary space (Bowers et al., 2005). We note that the TIP only investigates local properties about the singular point. More traditional adaptive dynamics analysis is needed to explore the global properties of the system.

The possibility of branching behavior in our model can be demonstrated from the TIP shown in Fig. 1. The plot shows the possibility of invasion of the mutant strain into the resident strain and vice versa. The curves giving the boundaries of the invasion domains have the same tangents at the point (D, λ)=(1, 2). If we choose a trade-off such that it is also tangential to the boundaries at this point, then (D, λ)=(1, 2) is a singular point of the system. The evolutionary behavior at the singularity can then be found by considering in which region the trade-off enters the singular point. In fact, Fig. 1 shows mutual invadability of a mutant strain into a resident strain, where the resident strain can be either the singular strain (D, λ) or a neighbor strain (D_1, λ_1). The invadability diagram is constructed in the (D_1, λ_1) plane where the different domains correspond to possible different invasion outcomes. A rare mutant strain (D_1, λ_1) can invade into the resident singular strain in the case where the mutant's fitness is larger than zero. By considering the growth rate of a mutant parasite strain, this gives the following condition of invadability by a non-singular strategy/strain:

$$g_1 = \lambda_1 S^*(D,\lambda) - D_0 - D_1 - m(D_1)P^*(D,\lambda) > 0, \tag{4}$$

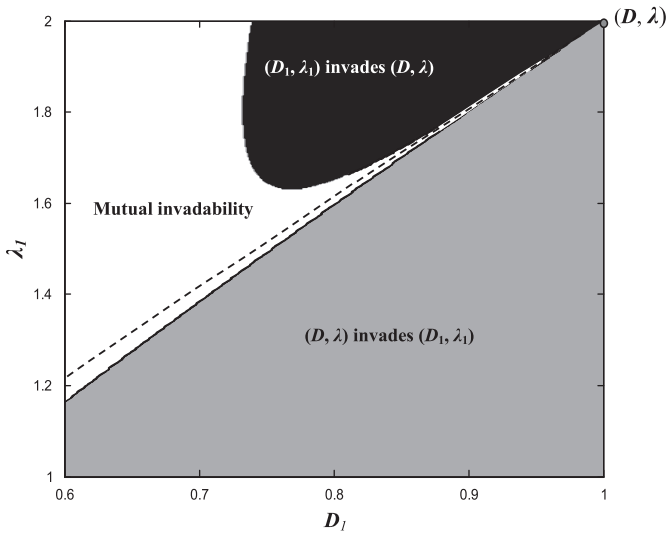

Fig. 1. A trade-off and invasion plot (TIP) of model (1)–(3) providing conditions for evolutionary branching. The trade-off function should be tangential to the evolutionarily singular point (λ, D). The branching behavior is observed for a trade-off function entering the point (λ, D) between the dashed-line curve and the upper boundary of the grey domain. For other details see the text. The parameters are K=2; k=0.2; D_0=0.2; δ=0.1; m_a=1.35; m_b=1.7; m_c=−1.5; r=2.

where g_1 is called the fitness of non-singular strategy (D_1, λ_1). The equilibrium densities S^* and P^* of species are given in Appendix A. The boundary of the invadability domain for strategy (D_1, λ_1) can be easily obtained from g_1=0 which gives

$$\lambda_1 = \frac{D_0 + D_1 + m(D_1)P^*(D,\lambda)}{S^*(D,\lambda)}. \tag{5}$$

We also consider the possibility of invasion of the singular strategy (λ, D) into nearby strategies (D_1, λ_1). The invasion fitness for the singular strategy is determined by

$$g = \lambda S^*(D_1,\lambda_1) - D_0 - D - m(D)P^*(D_1,\lambda_1), \tag{6}$$

where g is the fitness of the evolutionarily singular strategy invading the strategy (D_1, λ_1) at equilibrium. The boundary for the invadability conditions for (D, λ) can be determined by solving the equation g=0 with respect to λ_1. It can be done analytically based on the explicit equations for the stationary densities of S^* and P^* for the given functional dependence of the attack rate $m(D)$. Thus we need to specify the shape of the function $m(D)$. To reveal the type of the evolutionary singular strategy, however, we do not need to know the expression of $m(D)$ within the whole range of D. We only need to know the behavior of this function in the vicinity of the evolutionary singular point. We thus implement the 'local' approach. For this purpose we can consider (without the loss of generality) the Taylor expansion in the vicinity of D given by

$$m(D_1) \approx m_a + m_b(D_1 - D) + m_c\frac{(D_1 - D)^2}{2}, \tag{7}$$

where the coefficients m_i (i=a, b, c) are the certain parameters, $m_a > 0$, $m_b > 0$. In this case, the boundary of invadability for the singular strategy can be explicitly computed (see Appendix B); however, the obtained expressions are rather cumbersome. We denote the boundary for invadability conditions of (D, λ) into (D_1, λ_1) by

$$\tilde{\lambda}_1 = \tilde{\lambda}_1(D_1) \tag{8}$$

We plot the invadability boundaries based on numerical methods and the resultant diagram is shown in Fig. 1. This figure provides an example of the scenario where the evolutionarily

singular strategy can be a branching point, depending on the shape of the functional response. The diagram is constructed for the following model parameters: $K=2$; $k=0.2$; $D_0=0.2$; $\delta=0.1$; $m_a=1.35$; $m_b=1.7$; $m_c=-1.5$; $r=2$ and the evolutionarily singular point is $(D=1;\ \lambda=2)$. In Fig. 1, the grey color denotes the domain where only the singular strain (D, λ) can invade the other strains, but the other strains (when rare) cannot invade the evolutionarily singular strain. The black color shows the domain where the neighbor strains can invade the singular strain (D, λ). Finally, the white domain depicts the situation where both strains (D, λ) and (D_1, λ_1) can invade when rare (mutual invadability domain). Note that at an evolutionarily singular point (D, λ) the first derivatives $\lambda_1'(D_1)$ and $\tilde{\lambda}_1'(D_1)$ should always coincide and the slope of the trade-off function $\lambda(D)$ should be the same (Bowers et al., 2005). The dashed-line curve in the Fig. 1 is a parabolic function defined by the condition $2\lambda''(D)=\lambda_1''(D)+\tilde{\lambda}_1''(D)$ for the curvature and depicts the boundary for the branching behavior of the singularity point (see next paragraph).

From Fig. 1 it can be seen (see Bowers et al. (2005) for more detail) that depending on the shape of trade-off curve we can have three different outcomes. First, the singular point can be a repellor; in this case the trade-off curve should enter this point above the dashed line curve. Second, the singular point can be the evolutionary attractor; in this case the trade-off function should enter this point in the grey domain. Thirdly, the singular point would be a branching point in the case the trade-off curve enters this point below the dashed curve and above the grey domain. This follows from the property that to have a branching point the second derivative of trade-off curve $\lambda(D)$ should satisfy the following condition $2\lambda''(D)<\lambda_1''(D)+\tilde{\lambda}_1''(D)$ (for details see Bowers et al. (2005)). Our computation for parameters from Fig. 1 shows that $\lambda_1'(1)=\tilde{\lambda}_1'(1)=1.944; \tilde{\lambda}_1''(D)\approx -0.72; \lambda_1''(D)\approx 0.15$. Thus, to guarantee the evolutionarily branching the trade-off function should satisfy $-0.28>\lambda_1''(1)>-0.72$ with the gradient $\lambda'(1)=1.944$.

Interestingly, in the absence of a predator ($P\equiv 0$) evolutionary branching in the given model is impossible. Indeed, computation of the boundary of the invadability domain for strategy (D_1, λ_1) gives the same curve as for the boundary for invadability conditions of (D, λ) into (D_1, λ_1): $\lambda_1(D_1)\equiv\tilde{\lambda}_1(D_1)=\lambda(D_0+D_1)/(D+D_0)$. Thus, the existence of the mutual invadability domain on the TIP plot becomes impossible. The same holds true for the case where the density of predator is constant $P=P_0=const$ even if the attack rate is a function of the virulence $m=m(D)$; similar reasoning tells us that $\lambda_1(D_1)\equiv\tilde{\lambda}_1(D_1)$.

To explicitly show an example of evolutionary branching we choose realization of the trade-off relation given by the following hyperbolic parameterization:

$$\lambda(D)=\lambda_{\max}-(\lambda_{\max}-\lambda_{\min})\frac{1-(D-D_{\min}/D_{\max}-D_{\min})}{1+\varepsilon(D-D_{\min}/D_{\max}-D_{\min})} \tag{9}$$

where $D_{\min}$, $D_{\max}$ and $\lambda_{\min}$, $\lambda_{\max}$ are, respectively, the maximal and the minimal values of virulence and transmission rates, ε being a control parameter. We have chosen parameters that satisfy the above branching conditions from the TIP in Fig. 1.

Fig. 2A shows the evolutionary trajectory of parasite virulence in the 'evolutionary time' based on numerical simulations (see Appendix C for details). The simulation shows the parasite initially converging to the singular point at $(D, \lambda)=(1, 2)$ before branching into two distinct, coexisting strains. We show the trajectory in the vicinity of the singular point since a further evolutionary dynamics is determined by a choice of shape of $m(D)$ for large and small D. In the case, were $m(D)$ given by the parabolic function (7) the two branches will eventually evolve to the minimal and the maximal possible values of virulence given by $D_{\min}$ and $D_{\max}$. For more complex parameterization of $m(D)$ the two strains may evolve to some intermediate values of D lying between $D_{\min}$ and $D_{\max}$. For instance, in the case where we add the term $m_d(D_1-D)^4$ into expression (7) the strains after branching will adopt new continuously stable strategies (which are convergent stable and evolutionarily stable) characterized by the virulence $D_{01}=0.85$ and $D_{02}=1.13$ (for $m_d=1.25$) which are clearly located between $D_{\min}=0.5$ and $D_{\max}=1.25$. For brevity we do not show here the corresponding simulation diagrams.

Another important insight into the branching behavior can be found by using a PIP (pairwise invasion plot) representation which shows the evolutionary outcome for a specified trade-off function (Geritz et al., 1998; Dieckmann, 2002). The PIP shown in Fig. 2B represents the evolutionary outcome for the same

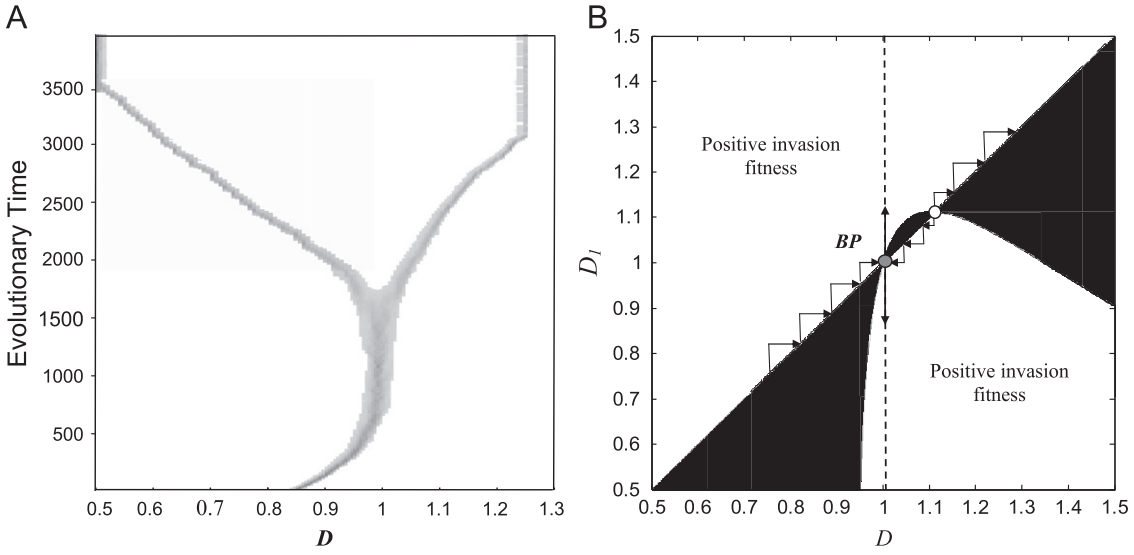

Fig. 2. (A) Numerical simulation of the branching process. The model parameter values are as in Fig. 1, with a trade-off function $\lambda(D)$ given by (9) with $D_{\min}=0.5$; $D_{\max}=1.25$, $\lambda_{\min}=0.9586$, $\lambda_{\max}=2.47$; the control parameter $\varepsilon=0.108$.This yields a gradient $\lambda'(D)=1.9435$ at $D=1$ and the curvature at the singular point $\lambda''(D)\approx -0.52$ as required for branching. The shading indicates the density of hosts infected by each parasite strain. The two strains will eventually evolve to the minimal and the maximal possible values of virulence: $D_{\min}$ and $D_{\max}$. (B) Pairwise invasibility plot (PIP) corresponding to the simulation in panel (A); mutant fitness is plotted as a function of the virulence of resident and mutant strains. The two evolutionarily singular strategies are the branching point (*BP*) shown by a grey filled circle and a repeller point shown by the open circle. Evolution of small mutations is shown by arrows and takes place along the diagonal.

trade-off function as was used to simulate the trajectory in Fig. 2A. In this figure, the white domain depicts the positive fitness of a rare mutant strain relative to the resident strategy; the black domain corresponds to negative fitness of mutant. Evolution of small mutations is schematically shown by arrows; a mutant strategy can invade only if its fitness is positive, thus the selection takes place as a sequence of successful mutations and substitutions. One can see from the figure that there are two evolutionarily singular strategies shown by the filled grey and open circles. The open circle represents the evolutionary repeller: as a sequence of mutations/substitutions the initial virulence will evolve away from this point, which is shown by arrows. The filled grey circle is the branching point corresponding to that of Fig. 2A: the selection will drive the virulence to the singularity (marked by a dashed line); however, this state is not stable and mutants have higher and lower positive fitness which will eventually lead to a disruptive selection (dimorphism) which is shown by bold vertical arrows.

Finally, we should mention that the apparent 'unlimited' growth of virulence on the right-hand side of the evolutionary repeller in Fig. 2B is an artifact of the use of (7) or (9), which gives only an approximation of the attack rate in the vicinity of the branching point. In the case, we consider $m(D)$ for large D we need to take into account saturation of the attack rate, which can be done, for instance, by using parameterization similar to (9). Our preliminary investigation reveals that for a certain large D there will be an evolutionary attractor (not shown). Thus, the presence of a predator would lead to a particularly interesting evolutionary bistability in terms of evolutionary states; depending on the initial value, the virulence can evolve either to the branching point with a further evolutionary disruption (dimorphic state) or it can progress up to a highly virulent strain (monomorphic state). A more thorough investigation of such bistability cases should clearly be a topic of further studies since the 'global' evolutionary behavior strongly would depend on a concrete choice of trade-off functions.

4. Effects of environmental properties on evolutionary branching

Note that the evolutionary branching behavior shown in Figs. 1 and 2 is not restricted to a particular set of model parameters. For instance, we found qualitatively similar behavior for other combinations of the attack rate parameters m_a, m_b, m_c as well as other ecological life-history traits (e.g., K, r). In Fig. 3A, B, and C we show the (m_a, m_b) parametric diagram where domain 1 corresponds to the possibility of the evolutionarily branching in the system; for the parameters from this domain there always exits a trade-off function resulting in branching at point (D, λ) and the corresponding TIP plot will be similar to that of Fig. 1. The three first diagrams in Fig. 3(A, B, and C) are plotted for different combinations of intrinsic birth rate r and the carrying capacity K. This allows us to estimate the possible influence of properties of the environment on the possibility of evolutionary branching (see discussion at the end of this section). For the parameters in domain 2 evolutionary branching is impossible for any shape of trade-off function. The corresponding TIP plot is shown in Fig. 3D.

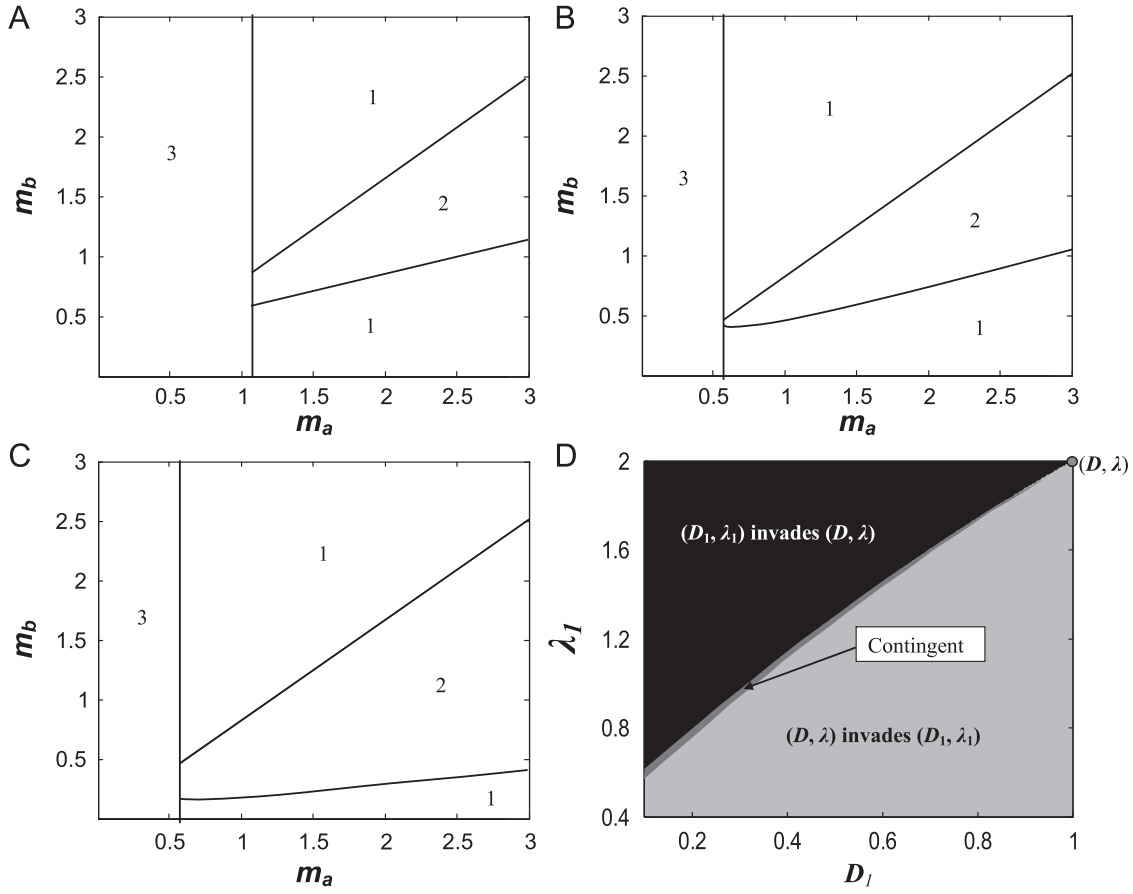

Fig. 3. Influence of ecosystem's eutrophication on the possibility of evolutionary branching. (A) $r=2$; $K=2$; (B) $r=2$; $K=15$ (large carrying capacity); (C) $K=2$; $r=7$ (high intrinsic prey birth rate). In each diagrams evolutionary branching can be possible only in domain 1. The meaning of the other domains is explained in the text. (D) A typical TIP (trade-off and invasion plot) corresponding to domain (2) in panels (A)–(C), where evolutionary branching is impossible (constructed for $m_a=2$; $m_b=1$; $r=2$; $K=2$). The meaning of the domains in the TIP is explained in the text. The other parameters are as in Fig. 1.

As in Fig. 1, the meaning of the grey and the black invadability domains are the same. However, the mutual invadability domain is now absent in the vicinity of the singular point. Instead, a dark grey domain appears corresponding to the situation where neither singular nor mutant strategy can invade into each other (Bowers et al., 2005). Thus, the singular stationary state can be an evolutionary attractor or repeller. Finally for parameters in domain 3 in Fig. 3A, B, and C, the coexistence of species S, I, P becomes impossible resulting in negative densities for some of species.

From the above (m_a, m_b) diagrams one can see that the dependence of evolutionary outcomes on those parameters is non-monotone. For a fixed m_a, evolutionary branching is possible either for small m_b or for large m_b. This means that sensitivity of the attack rate to predation on infected hosts should be either small or large to provide such behavior. For small values of m_a (domain 3), the coexistence of species becomes unfeasible; the attack rate of the predator is too small to maintain its population alive. Variation of the parameter m_c does not qualitatively change the above results.

It will be interesting to make some predictions regarding the properties of the environment where we should expect to observe the evolutionary branching in a prey–pathogen–predator system. The ultimate conclusions would be largely dependent on the shape of trade-off functions that should be typical for a particular natural environment (in the case such functions exist in reality). Here we can provide only an insight into this issue by estimating the feasibility of branching behavior in an environment with different amounts of available food resources as well as different values for the growth rate of prey. This can be modeled by varying the parameters K and r. Fig. 3B shows variation of the initial (m_a, m_b) diagram in the case of an increase in resource availability (large K). One can easily see that overall the size of the 'branching' domain increases. In particular, branching becomes possible for smaller attack rates of predator. The increase in the *per capita* birth rate of prey (for the constant total amount of resources K) enhances the possibility of branching in the case of high sensitivity of the attack rate to the virulence of the disease (the upper part of domain 1 grows in size). However, in the case of small sensitivity of the attack rate to the virulence (small m_b), the increase in r would impede the evolutionary branching.

Finally, we should note that the above results are not limited to the given values of the evolutionary singular strategy ($D=1$, $\lambda=2$). We found qualitatively similar results on the branching behavior in model (1)–(3) within a large range of parameters for other possible combinations of (D, λ).

5. Discussion and conclusions

Understanding the factors promoting diversity of pathogen strains in wild populations is crucial to our management of a range of natural disease systems. Classic host–parasite theory contends that coexistence of parasite strains is prevented due to a competitive exclusion principle, with the strain which maximizes the epidemiological R_0 outcompeting all other strains (Bremmerman and Thieme, 1989). However, subsequent theory has identified a variety of mechanisms which may allow for multiple parasite strains to arise and coexist, including density-dependence of the host mortality (Pugliese, 2002; Svennungsen and Kisdi, 2009; Best et al., 2009), superinfection (Adler and Mosquera, 2002; Boldin and Diekmann, 2008), and specialist parasitism against multiple hosts (Regoes et al., 2000; Gudelj et al., 2004; Best et al., 2010). Here, we have identified a further mechanism allowing for a dimorphism in parasite virulence to arise through evolutionary branching, namely the presence of a predator. Crucially, we found that the predator in the system should be dynamic, i.e. to have non-constant density, and should be selective in consuming prey infected with more virulent parasites (see Section 3 for details).

Our assumption that prey infected with more virulent parasites are at greater risk of predation is somewhat intuitive, since we may assume that such prey will suffer more severe disease symptoms and reduced fitness, and thus be less able to escape from predator attack (Choo et al., 2003). There is also some empirical evidence for this assumption. For example, in their classic study on parasites in Red Grouse populations, Hudson et al. (1992) found that birds killed by predators carried significantly higher parasite burdens than those killed during the shooting season. It may reasonably be assumed that greater parasite loads correlate with greater disease virulence, thus supporting our assumption. There are also many examples of parasites that manipulate the behavior of an intermediate host (i.e. the prey) for an increased chance of reaching their definitive host (i.e. the predator; Lafferty, 1999). Although we have not considered this particular scenario explicitly here, such parasites may also play a role in making infected prey more vulnerable to predation. Overall, there is a large body of evidence that predators target infected rather than healthy prey (Hatcher et al., 2006 and the references therein, Duffy and Sivars-Becker, 2007), however, it is still unclear from these studies whether they target more infected prey. We believe that a proper empirical insight into this issue would be extremely beneficial for a further understanding of evolution of virulence in wildlife. Our results suggest that we should also expect greater diversity in parasite strains in such host populations that are also at risk of predation than in populations with little or no pressure from predators.

The vast majority of host–parasite theory has focused on the case of one host and one parasite interacting, using the classic SIR-type framework. Whilst this assumption allows for easier analysis and increased tractability, ecological systems are generally much more complex, with a variety of interactions between species at different trophic levels. There are a growing number of studies examining host and parasite evolution where there are multiple host or parasite strains present (Regoes et al., 2000; Ganusov et al., 2002; Gudelj et al., 2004; see also Best et al., 2009, 2010). However, there has been very little account of the impact of species at different trophic levels on host–parasite interactions. Those studies that do exist (Choo et al., 2003; Morozov and Adamson, 2011) have found that the selection pressure on parasite virulence is strongly impacted by the presence of a predator. Here, we have also shown that the presence of a predator can fundamentally alter the possible evolutionary dynamics of parasite virulence. Clearly for more accurate predictions on the evolution of virulence it is vital that we gain a greater understanding of the links between different species in natural systems.

It is well understood that the form of the trade-offs assumed in evolutionary models is crucial to the predicted outcome. Much recent theory has been dedicated to developing geometric analysis techniques that highlight which shapes of trade-offs result in which evolutionary behaviors (de Mazancourt and Deickmann, 2004; Rueffler, 2004; Bowers et al., 2005; Kisdi, 2006; Svennungsen and Kisdi, 2009). Here we have used trade-off and invasion plots (TIPs; Bowers et al., 2005) to show that branching may occur for 'weakly' concave trade-offs between parasite transmission and virulence (i.e. $\lambda''(D)<0$). Our results therefore fit with the classic assumption in the literature that transmission should be a saturating (concave) function of virulence (see Alizon et al. (2009)). We therefore do not require 'exotic' trade-off functions, where the trade-off must be locally convex, for evolutionary branching to occur (e.g., Svennungsen and Kisdi, 2009), but instead we suggest that polymorphisms in virulence may occur for a range of realistic trade-offs between transmission and virulence.

We have found that evolutionary branching is possible for a large range of ecological parameters (life history traits). A necessary condition of evolutionary branching in the model is that the predator consuming infected prey must be 'dynamic'; in the case where the predator density is included as a constant parameter, evolutionary branching is not observed for any trade-off relations $\lambda(D)$ and $m(D)$ (see Section 3). Similarly, it is necessary to have selective predation by discriminating between the infected prey with degree of different virulence, i.e. to have $m=m(D)$, and branching will not be observed in the model with a constant attack rate m. (here we consider that $\lambda(D)$ is a concave function, in this case the second derivative of the mutant fitness (4) with constant m will be always negative, thus the evolutionary singularity will be always an evolutionarily stable strategy, see Geritz et al. (1998)). Moreover, the selectivity gradient of predation at the evolutionary singular point given by $m'(D)\equiv m_b$ should be either rather steep (supercritical) or shallow (subcritical) (see Fig. 3A, B, and C). We have also found that the environmental conditions will play a role in determining the possibility of branching. In particular, we found that eutrophication of the ecosystem, resulting in an increase of the carrying capacity, would promote evolutionary branching of parasites/viruses. This conclusion may be of importance when comparing the biodiversity of marine viruses in water with a different degree of eutrophication (nutrient concentration in water) which is currently a topic of intense studies (Fuhrman, 1999; Wommack and Colwell, 2000; Dunigan, 2006).

Our key result, that evolutionary branching may occur in a simple SI model with the addition of a selective predator, appears to be reasonably robust to changes in the model structure. In particular, we found that making the model more 'realistic' by including the possibility of recovery by infected individuals back to susceptibility (SIS model) or allowing the predator to consume some susceptible individuals (see the electronic Supplementary material S1) does not alter the main results; the trophic interaction can still result in evolutionary branching of the pathogen's virulence.

Among future directions of research we would like to mention the following. Firstly, it will be important to investigate the evolutionary trajectory of both pathogen strains after the branching event, i.e. the behavior of the resultant dimorphic pathogen population. In the current study we mostly use the local approach (in terms of local derivatives of the trade-off functions) showing the existence of branching points. Further long-term coexistence of strains and the possibility of further branching (e.g. an evolutionary trimorphism) in the model remains an open question. Secondly, it will be important to include in the current model the possibility of sustained species oscillations (population cycles). This can be done, for instance by taking into account saturation in the functional response of predator. It was recently shown (Morozov and Adamson, 2011) that in the case where the population dynamics are cyclic, this can completely change the evolutionary outcomes compared to the regimes with stationary population densities. Finally, it will be important to consider the possibility of evolutionary branching in the case where the predator is generalist and not specialist as this may be a more accurate description of host–pathogen–predator interactions in certain systems (Hudson et al., 1998). Overall we conclude that both theoretical and empirical studies should take greater account of the complexity of ecological systems to fully understand the evolution of virulence.

Acknowledgments

We highly appreciate the three anonymous referees for their suggestions to improve the manuscript.

Appendix A

Here we briefly consider the dynamical properties of model (1)–(3). The model has the following stationary states.

1. The trivial stationary state (0,0,0). It is always unstable.
2. The disease free and predator-free state (K,0,0). It is locally stable for $D+D_0>K\lambda$.
3. The predator-free state (S^1, I^1, 0) with $S^1=(D+D_0)/\lambda$ and $I^1=r(K\lambda-D-D_0)/[\lambda(K\lambda+r)]$. This state is locally stable in the case $D+D_0<K\lambda$ and $\delta>km(D)I^1$.
4. The interior stationary state (S^*, I^*, P^*) with the species densities being positive. The equilibrium densities are determined by

$$S^*=\frac{rkKm(D)-(r+\lambda K)\delta}{rkm(D)}, \tag{A1}$$

$$I^*=\frac{\delta}{km(D)}, \tag{A2}$$

$$P^*=\frac{rk\delta m(D)-\lambda r\delta-\lambda^2\delta K-(D_0+D)rkm(D)}{rkm^2(D)}, \tag{A3}$$

We shall prove that in the case species densities (A1)–(A3) are positive, the interior stationary state (S^*, I^*, P^*) is globally stable. We use the following change of variables $I=i\lambda K/(\lambda K+1)$ and $P=pk\lambda K/(\lambda K+1)$ and re-write the initial model as

$$S'=r\left(1-\frac{S}{K}\right)S-\lambda Si, \tag{A4}$$

$$i'=(\lambda S-D_0-D-map)i, \tag{A5}$$

$$p'=(mai-\delta)p, \tag{A6}$$

where $a=k\lambda K/(\lambda K+1)$. Evidently, the existence of the interior stationary state of (1)-(3) signifies the existence of the interior stationary state of (A4)–(A6) and vice-versa.

For model (A4)–(A6) we consider the following positively definite Lyapunov function:

$$L=S-S^*-S^*\ln\left(\frac{S}{S^*}\right)+i-i^*-i^*\ln\left(\frac{i}{i^*}\right)+p-p^*-p^*\ln\left(\frac{p}{p^*}\right), \tag{A7}$$

where (S^*, i^*, p^*) are the stationary densities of the interior state of (A4)–(A5). We compute the time derivative of L

$$\frac{dL}{dt}=(S-S^*)\left(r\left(1-\frac{S}{K}\right)-\lambda i\right)+(i-i^*)(\lambda S-D_0-D-map)+(p-p^*)(mai-\delta)$$

After some simplification we obtain

$$\frac{dL}{dt}=-r(S-S^*)^2/K \tag{A8}$$

Thus, the Lyapunov function is negative everywhere except the line $S=S^*$. However, the only possible invariant set on $S=S^*$is the equilibrium (S^*, I^*, P^*). Thus, by applying the Lasalle's lemma (Alligood et al., 1997) we can conclude that the trajectory will eventually converge to the interior equilibrium, i.e. the interior stationary state is globally asymptotically stable.

Appendix B

Here we derive analytical expressions for the invasibility boundary $\tilde{\lambda}_1=\tilde{\lambda}_1(D_1)$ with the function $m(D_1)$ given by (7). By

equating the invasion fitness (6) to zero and substituting (7) we obtain the following quadratic equation:

$$A\tilde{\lambda}_1^2 + B\tilde{\lambda}_1 + C = 0, \quad \text{(B1)}$$

where the coefficients A, B, C are given by

$$A = \frac{K\delta m_a}{krm(D_1)}, \quad B = \frac{\delta - kKm(D_1)}{km^2(D_1)} m_a - \frac{\lambda\delta K}{krm(D_1)}$$

$$C = \frac{kKm(D_1) - \delta}{km(D_1)}\lambda + \frac{D_1 + D_0}{m(D_1)} m_a - (D + D_0)$$

Evidently, the solution of (B1) is determined by the following expression which gives two branches of the curve:

$$\tilde{\lambda}_1 = \frac{-B \pm \sqrt{B^2 - 4AC}}{2A}. \quad \text{(B2)}$$

For the branch entering the point (D, λ) one should choose the sign '$-$' in front of the square root.

Appendix C

Here we provide details on simulation of the evolutionary trajectory shown in Fig. 2A.

The simulations are performed in the C programming language. $N=101$ possible parasite strains are defined along the trade-off from $D_{\min}=0.25$ to $D_{\max}=1.25$, $\lambda_{\min}=0.378$, $\lambda_{\max}=2.47$, $\varepsilon=0.15$ creating 101 potential infected prey strains. All but one of the infected strains are initialized at zero density, with the remaining (initial) infected prey, and the susceptible prey and predator, given a positive density. The population dynamics (i.e. Eqs. (1)–(3)) are then numerically solved using a 4th order Runge–Kutte routine for large time such that the system will be near its dynamic attractor (stationary state). A neighboring 'mutant' infected strain—either one higher or lower than the current 'resident'—is then initialized at a low density (10% of the resident strain density), and the population dynamics are then run again. At each 'evolutionary' time step, any strains whose density has fallen below some threshold (0.0001) are presumed extinct and their density set to zero, and the mutation routine is implemented (note when multiple 'resident' infected strains are present, the mutating strain is chosen by a density-weighted probability of the current residents). By repeating this process the evolutionary trajectory as seen in Fig. 2A is built up.

Appendix D. Supplementary material

Supplementary data associated with this article can be found in the online version at http://dx.doi.org/10.1016/j.jtbi.2012.04.023.

References

Adler, F.R., Mosquera Losada, J., 2002. Super- and coinfection: filling the range. In: Dieckman, U., Metz, J.A.J., Sabelis Maurice, W., Sigmund, K. (Eds.), Adaptive Dynamics of Infectious Diseases: In Pursuit of Virulence Management. Cambridge University Press, Cambridge, pp. 138–149.

Alizon, S., Hurford, A., Mideo, N., van Baalen, M., 2009. Virulence evolution and the trade-off hypothesis: history, current state of affairs and future. J. Evol. Biol. 22, 245–259.

Alligood, K.T., Yorke, J.A., Sauer, T.D., 1997. Chaos: An Introduction to Dynamical Systems. Springer.

Anderson, R.M., May, R.M., 1982. Coevolution of hosts and parasites. Parasitology 85, 411–426.

Best, A., White, A., Boots, M., 2009. The implications of coevolutionary dynamics to host–parasite interactions. Am. Nat. 173, 779–791.

Best, A., White, A., Kisdi, E., Antonovics, J., Brockhurst, M., Boots, M., 2010. The evolution of host–parasite range. Am. Nat. 176, 63–71.

Boldin, B., Diekmann, O., 2008. Superinfections can induce evolutionarily stable coexistence of pathogens. J. Math. Biol. 56, 635–672.

Bremermann, H.J., Pickering, J., 1983. A game-theoretical model of parasite virulence. J. Theor. Biol. 100, 411–426.

Bremermann, H.J., Thieme, H.R., 1989. A competitive exclusion principle for pathogen virulence. J. Math. Biol. 27, 179–190.

Bowers, R.G., Hoyle, A., White, A., Boots, M., 2005. The geometric theory of adaptive evolution: trade-off and invasion plots. J. Theor. Biol. 233, 363–377.

Choo, K., Williams, P.D., Day, T., 2003. Predation, host mortality, and the evolution of virulence. Ecol. Lett. 6, 310–315.

Day, T., Proulx, S.R., 2004. A general theory for the evolutionary dynamics of virulence. Am. Nat. 163, 40–63.

de Mazancourt, C., Dieckmann, U., 2004. Trade-off geometries and frequency-dependent selection. Am. Nat. 164, 765–778.

Dieckmann, U., 2002. Adaptive dynamics of pathogen–host interactions. In: Dieckmann, U., Metz, J.A.J., Sabelis, M.W., Sigmund, K. (Eds.), Adaptive Dynamics of Infectious Diseases: Pursuit of Virulence Management. Cambridge University Press, pp. 39–59.

Dunigan, D.D., Fitzgerald, L.A., Van Etten, J.L., 2006. Phycodnaviruses: a peek at genetic diversity. Virus Res. 117, 119–132.

Duffy, M.A., Sivars-Becker, L., 2007. Rapid evolution and ecological host–parasite dynamics. Ecol. Lett. 10, 44–53.

Ebert, D., Weisser, W.W., 1997. Optimal killing for obligate killers: the evolution of life histories and virulence of semelparous parasites. Proc. R. Soc. B 268, 2331–2337.

Friend, M., 2002. Avian disease at the Salton Sea. Hydrobiologia 473, 293–306.

Friman, V.-P., Lindstedt, C., Hiltunen, T., Laakso, J., Mappes, J., 2009. Predation on multiple trophic levels shapes the evolution of pathogen virulence. PLoS ONE 4 (8), 6761.

Fuhrman, J.A., 1999. Marine viruses and their biogeochemical and ecological effects. Nature 399, 541–548.

Ganusov, V., Bergstrom, C., Antia, R., 2002. Within-host population dynamics and the evolution of microparasites in a heterogeneous host population. Evolution 56, 213–223.

Geritz, S.A.H., Kisdi, E., Meszéna, G., Metz, J.A.J., 1998. Evolutionarily singular strategies and the adaptive growth and branching of the evolutionary tree. Evol. Ecol. 12, 35–57.

Gudelj, I., van den Bosch, F., Gilligan, C.A., 2004. Transmission rates and adaptive evolution of pathogens in sympatric heterogeneous plant populations. Proc. R. Soc. B 271, 2187–2194.

Hatcher, M.J., Dick, J.T.A., Dunn, A.M., 2006. How parasites affect interactions between competitors and predators. Ecol. Lett. 9, 1–19.

Holmes, J.C., Zohar, S., 1990. Pathology and behavior. In: Barnard, C.J., Behnke, J.M. (Eds.), Parasitism and Host Behavior. Taylor and Francis, London, pp. 34–63.

Hoyle, A., Bowers, R.G., White, A., Boots, M., 2008. The influence of trade-off shape on evolutionary behaviour in classical ecological scenarios. J. Theor. Biol. 250, 498–511.

Hudson, P.J., Dobson, A.P., Newborn, D., 1992. Do parasites make prey vulnerable to predation? Red grouse and parasites. J. Anim. Ecol. 61, 681–692.

Hudson, P.J., Dobson, A.P., Newborn, D., 1998. Prevention of population cycles by parasite removal. Science 282, 2256–2258.

Johnson, P.T.J., Stanton, D.E., Preu, E.R., Forshay, K.J., Carpenter, S.R., 2006. Dining on disease: how interactions between infection and environment affect predation risk. Ecology 87, 1973–1980.

Kabata, Z., 1985. Parasites and Diseases of Fish Cultured in the Tropics. Taylor & Francis, London.

Kisdi, E., 2006. Trade-off geometries and the adaptive dynamics of two co-evolving species. Evol. Ecol. Res. 8, 959–973.

Lafferty, K.D., 1999. The evolution of trophic transmission. Parasitol. Today 15, 111–115.

Metz, J.A.J., Nisbet, R.M., Geritz, S.A.H., 1992. How should we define "fitness" for general ecological scenarios? Trends Ecol. Evol. 7, 198–202.

Morozov, A., Adamson, M., 2011. Evolution of virulence driven by predator–prey interaction: possible consequences for population dynamics. J. Theor. Biol. 276, 181–191.

Packer, C., Holt, R.D., Hudson, P.J., Lafferty, K.D., Dobson, A.P., 2003. Keeping the herds healthy and alert: implications of predator control for infectious disease. Ecol. Lett. 6, 797–802.

Pugliese, A., 2002. On the evolutionary coexistence of parasite strains. Math. Biosci. 177–178, 355–375.

Regoes, R.R., Nowak, M.A., Bonhoeffer, S., 2000. Evolution of virulence in a heterogeneous host population. Evolution 54, 64–71.

Rueffler, C., Van Dooren, T.J.M., Metz, J.A.J., 2004. Adaptive walks on changing landscapes: Levins' approach extended. Theor. Popul. Biol. 65, 165–178.

Svennungsen, T., Kisdi, E., 2009. Evolutionary branching of virulence in a single-infection model. J. Theor. Biol. 257, 408–418.

Taylor, D.R., Jarosz, A.M., Lenski, R.E., Fulbright, D.W., 1998. The acquisition of hypovirulence in host–pathogen systems with three trophic levels. Am. Nat. 151, 343–355.

Wommack, K.E., Colwell, R.R., 2000. Virioplankton: viruses in aquatic ecosystems. Microbiol. Mol. Biol. Rev. 64, 69–114.